THE JOURNAL OF BIOLOGICAL CHEMISTRY
Vol. 279, No. 5, Issue of January 30, pp. 3651–3661, 2004
Printed in U.S.A.

Evidence for Antagonistic Regulation of Cell Growth by the Calcineurin and High Osmolarity Glycerol Pathways in *Saccharomyces cerevisiae**

Received for publication, June 10, 2003, and in revised form, October 9, 2003
Published, JBC Papers in Press, October 28, 2003, DOI 10.1074/jbc.M306098200

Atsunori Shitamukai‡, Dai Hirata, Shinya Sonobe, and Tokichi Miyakawa§

From the Department of Molecular Biotechnology, Graduate School of Advanced Sciences of Matter, Hiroshima University, Higashi-Hiroshima 739-8530, Japan

Because Ca^{2+} signaling of budding yeast, through the activation of calcineurin and the Mpk1/Slt2 mitogen-activated protein kinase cascade, performs redundant function(s) in the events essential for growth, the simultaneous deletion of both these pathways (Δ*cnb1* Δ*mpk1*) leads to lethality. A *PTC4* cDNA that encodes a protein phosphatase belonging to the PP2C family was obtained as a high dosage suppressor of the lethality of Δ*cnb1* Δ*mpk1* strain. Overexpression of *PTC4* led to a decrease in the high osmolarity-induced Hog1 phosphorylation, and *HOG1* deletion remarkably suppressed the synthetic lethality, indicating an antagonistic role of the high osmolarity glycerol (HOG) pathway and the Ca^{2+} signaling pathway in growth regulation. The calcineurin-Crz1 pathway was required for the down-regulation of the HOG pathway. Analysis of the time course of actin polarization, bud formation, and the onset of mitosis in synchronous cell cultures demonstrated that calcineurin negatively regulates actin polarization at the bud site, whereas the HOG pathway positively regulates bud formation at a later step after actin has polarized.

Cells of the yeast *Saccharomyces cerevisiae* evaluate and cope with their external environment by using rapidly responding, highly complex signaling pathways. Of particular importance are the signaling pathways known collectively as the mitogen-activated protein kinase (MAPK)[1] cascade, which couples an extracellular input signal to a variety of outputs. The budding yeast possesses five MAPKs acting in five functionally distinct cascades, each mediating physiologically distinct responses (1). Adaptation to high osmolarity is mediated by the HOG (high osmolarity glycerol) pathway, in which the Hog1 MAPK cascade couples the high osmolarity signal to glycerol accumulation. The Hog1 MAPK of this pathway is related to the members of the family of human stress-activated p38 MAPKs. The activation of the HOG pathway is regulated by bifurcated upstream branches, one mediated by the Sho1 sensor and the other by the two-component system consisting of Sln1, Ypd1, and Ssk1 (2–6). The HOG pathway is negatively regulated by Ptp2 and -3, which are protein-tyrosine phosphatases, and by Ptc1, -2, and -3 serine/threonine-protein phosphatases belonging to the PP2C family (3, 7–9). The HOG pathway regulates various stress genes for osmoprotection including *GPD1*, which encodes glycerol-3-phosphate dehydrogenase, an enzyme involved in glycerol synthesis (10). This pathway is also suggested to be involved in the regulation of the cell cycle, budding pattern, and cell division after osmotic stress. However, the details of the regulatory mechanisms of these events are unknown (11, 12).

In contrast to the HOG pathway, the Pkc1-Mpk1/Slt2 MAPK cascade responds to low osmolarity conditions. An important function of the Pkc1 pathway is to maintain cell wall integrity in response to low osmolarity and high temperature conditions by controlling the assembly of the cell wall (1).

Another major mechanism for adaptation to environmental changes in yeast is Ca^{2+} signaling. Calcineurin, essential only under specific environmental conditions, is an important mediator of the Ca^{2+} signal. Calcineurin is required for the recovery from the G_1 arrest induced by mating pheromones and for homeostasis of ions, including Na^+/Li^+, Mn^{2+}, and OH^- (13–16). Calcineurin regulates the expression of ion transporter genes by a mechanism mediated by Crz1, a calcineurin-dependent transcription factor (17, 18).

Although the defect of either calcineurin or the Mpk1 MAPK cascade alone does not lead to lethality under normal conditions, simultaneous defects of these pathways are synthetically lethal, indicating that the two pathways perform redundant function(s) in same essential event(s) for cell growth (19, 20). Upon activation by Ca^{2+} or various stimuli, the Mpk1 MAPK cascade maintains cell wall integrity by controlling the cell wall (1). In addition to these mechanisms, the two signaling pathways coordinately regulate the G_2-M transition through the activation of Swe1, a negative regulator of Cdc28/Clb in the G_2 phase (21). In this process, calcineurin up-regulates Swe1 function in two ways, one by the activation of the transcription of *SWE1* gene and the other by the destabilization of Hsl1 kinase, a negative regulator of Swe1 kinase. A high concentration of $CaCl_2$ in the medium causes the cells to activate these pathways and leads the cells to a G_2 cell-cycle delay. It was proposed that the activation of these pathways occurs in response to a membrane stretch stress (21).

In this present report, we show that the HOG pathway and the Ca^{2+} signaling pathways antagonize one another in the regulation of cell growth. We further demonstrate that these pathways are antagonistic in the regulation of bud emergence. In the presence of $CaCl_2$ in the medium, the activation of

* This work was supported in part by Grants-in-aid for Scientific Research 10460044, 11556017, and 14206012 (to T. M.) from the Ministry of Education, Science, Culture, Arts, and Sports of Japan. The costs of publication of this article were defrayed in part by the payment of page charges. This article must therefore be hereby marked "*advertisement*" in accordance with 18 U.S.C. Section 1734 solely to indicate this fact.

‡ Recipient of a Japan Society of the Promotion of Science fellowship (DC1).

§ To whom correspondence should be addressed. Tel.: 81-824-24-7763; Fax: 81-824-24-7045; E-mail: tmiyaka@hiroshima-u.ac.jp.

[1] The abbreviations used are: MAPK, mitogen-activated protein kinase; DTT, dithiothreitol; PMSF, phenylmethylsulfonyl fluoride; MBP, myelin basic protein; HA, hemagglutinin; WT, wild type; HOG, high osmolarity glycerol.

TABLE I
Yeast strains used in this study

Strain	Genotype	Source
W303–1A	*MAT***a** *ade2–1 his3–11, 15 leu2–3, 112 trp1–1 ura3–1 can1–100*	From Dr Rothstein
YAT1	*MAT***a** Δ*zds1*::*TRP1*	(21)
DTH14	*MAT***a** Δ*cnb1*::*HIS3*	(21)
TNP36	*MAT***a** Δ*cnb1*::*HIS3* Δ*mpk1*::*HIS3*	(20)
TNP46	*MAT***a** Δ*mpk1*::*HIS3*	(21)
SOS5	*MAT***a** Δ*hog1*::*TRP1*	This study
SOS27	*MAT***a** Δ*hog1*::*TRP1* Δ*mpk1*::*HIS3*	This study
SOS31	*MAT***a** Δ*hog1*::*TRP1* Δ*cnb1*::*HIS3*	This study
SOS44	*MAT***a** Δ*hog1*::*TRP1* Δ*swe1*::*HIS3*	This study
SOS48	*MAT***a** Δ*hog1*::*TRP1* Δ*mpk1*::*HIS3* Δ*cnb1*::*URA3*	This study
SHI26	*MAT***a** Δ*swe1*::*HIS3*::*SWE1–9myc*::*URA3*	This study
SHI27	*MAT***a** Δ*hog1*::*TRP1* Δ*swe1*::*HIS3*::*SWE1–9myc*::*URA3*	This study
SHI30	*MAT***a** Δ*hog1*::*TRP1* Δ*cnb1*::*HIS3* Δ*swe1*::*HIS3*::*SWE1–9myc*::*URA3*	This study
SHI63	*MAT***a** Δ*cnb1*::*HIS3* Δ*swe1*::*HIS3*::*SWE1–9myc*::*URA3*	This study
SHI132	*MAT***a** Δ*crz1*::*TRP1*	M. Mizunuma
SHI119	*MAT***a** Δ*hog1*::*TRP1*::*3HA-HOG1*::*URA3*	This study
SHI121	*MAT***a** Δ*cnb1*::*HIS3* Δ*hog1*::*TRP1*::*3HA-HOG1*::*URA3*	This study
SHI288	*MAT***a** Δ*crz1*::*TRP1* Δ*hog1*::*TRP1*::*3HA-HOG1*::*URA3*	This study
SHI290	*MAT***a** *ura3*::*GAL1-CMP2ΔC*::*URA3*	M. Mizunuma
SHI318	*MAT***a** Δ*cnb1*::*HIS3* Δ*pbs2*::*URA3* Δ*hog1*::*TRP1*::*3HA-HOG1*::*URA3*	This study
SHI131	*MAT***a** Δ*ste11*::*URA3* Δ*cnb1*::*HIS3* Δ*hog1*::*TRP1*::*3HA-HOG1*::*URA3*	This study
SHI313	*MAT***a** Δ*ssk1*::*URA3* Δ*cnb1*::*HIS3* Δ*hog1*::*TRP1*::*3HA-HOG1*::*URA3*	This study
SH7687	*MAT***a** Δ*ptp2*::*CgHIS3*	(43)
SHI334	*MAT***a** Δ*cnb1*::*HIS3* Δ*ptp2*::*CgHIS3*	This study

calcineurin negatively regulates actin polarization at the bud site, whereas the HOG pathway promotes bud formation at a step after actin polarization. We also show that the calcineurin-Crz1 pathway is involved in the down-regulation of the HOG pathway activated by Ca^{2+} or hyperosmotic stress.

MATERIALS AND METHODS

Yeast Strains, Media, and Plasmids—Yeast strains used in this study are listed in Table I. All yeast strains were derivatives of W303. Media used were as described previously (21). *PBS2* and *SSK1* was deleted with the *pbs2*::*URA3* and *ssk1*::*URA3* fragment from pDBP22 and pDSS12 respectively (gift from T. Maeda). *STE11* was deleted with the *ste11*::*URA3* fragment from pNC202 (gift from R. Akada). The galactose-inducible *PTC1*, *PTC2*, and *PTC3* plasmids were used: YEplac195GAL-PTC1, YEplac112GAL-PTC2, and YEplac112GAL-PTC2, respectively (22). The SWE1-myc construct was generated as follows. The NheI site in the pSWE1–40 (23) containing GAL-SWE1-HA was converted to a XhoI site using the linker oligonucleotide 5′-CCTCGAGG-3′, and the XbaI-SalI fragment was cloned into pAS5, pUC119 plasmid containing 9 × Myc epitope tag and *TDH2* terminator. The HindIII-SphI fragment of pAS5 was cloned into HindIII-SphI-digested YIp5-SWE1-F, containing the sequences corresponding to the N terminus of *SWE1* gene and its own promoter generated by PCR using two oligonucleotides, 5′-TTTTGAATTCTAAATAGGTTCCAC-CTC-3′ and 5′-TTTTAAGCTTTCGAAGACGGAGAATCT-3′. To create the SWE1-myc strain SHI26, the construct was digested with PmaCI, which cuts the promoter of *SWE1*, directing integration at the *SWE1* locus in yeast. The 3HA-HOG1 construct was generated as follows. The *HOG1* promoter region with start codon was generated by PCR using two primers, pHOG1-HindIII (5′-TTTTAAGCTTGACCCATTCCGATT-T-3′) and pHOG1-ATG-NheI-BamHI (5′-TTTTGGATCCGCTAGCCAT-TATTATATACGA-3′), and cloned into HindIII/BamHI-digested pRS-315 plasmid (pRS315-HOG1-F). The *HOG1* coding region without start codon was generated by PCR using two primers, pHOG1-NheI (5′-TT-TTGCTAGCACCACTAACGAGGAA-3′) and pHOG1-XbaI (5′-TTTTTC-TAGATGCAAAAGACTAAA-3′), and cloned into NheI/XbaI-digested pRS315-HOG1-F plasmid. Next, the NheI-digested 3HA fragment was cloned into a NheI site of this plasmid. The resulting plasmid, pRS315–3HA-HOG1, fully complemented the osmosensitivity of the Δ*hog1* strain. This plasmid was digested with HindIII and XbaI and cloned into HindIII/NheI-digested YIp5. To create the HOG1-HA strain SHI119, the YIp5-HOG1–3HA was digested with Eco81I, which cuts the promoter of *HOG1*, directing integration at the *HOG1* locus in the Δ*hog1* strain.

The galactose-inducible *PTC4* plasmid, YEp51-PTC4, was generated by using two primers, pPTC4-N (5′-AAAAAGTCGACATGGGTCAATT-GCTTTCCC-3′) and pPTC4-C (5′-TTTTAAGCTTAGCGAAGAAGC-GAAGAAGAG-3′), and digested with SalI-HindIII and cloned into the SalI-HindIII-digested YEp51 vector.

Isolation of Suppressor cDNA Clones—The Δ*cnb1* Δ*mpk1* mutant (TNP36) was transformed with cDNA libraries constructed in the yeast expression vector pNV7, in which yeast cDNA sequences are placed under the control of the inducible *GAL1* promoter (gift from K. Matsumoto, Nagoya University, Nagoya, Japan) on selection plate (SD minus uracil) containing 1 M sorbitol. The transformants were screened for growth on YPG plate (without 1 M sorbitol). The 85 positive transformants were isolated from 35,000 transformants. Six cDNA, including *MPK1* gene, were isolated by the screening.

Cell-cycle Synchronization—The procedure for cell-cycle synchronization was described previously (21). Cells were grown in YPD to a density of 2–3 × 10^6 cells/ml at 28 °C. Synthetic α-factor was added to a final concentration of 5 μg/ml, and cells were incubated for 135 min. After washing the cells with ice-cold water to remove α-factor, the cells were suspended in fresh YPD or YPD containing $CaCl_2$.

Immunoblotting—The cells were washed with TEG buffer (50 mM Tris-HCl (pH 7.5), 10 mM EDTA, 5 mM EGTA, 25 mM NaCl, 0.05% Tween 20, and 10% glycerol) containing 1 mM dithiothreitol, phosphatase inhibitors (10 mM NaF and 1 mM sodium orthovanadate), and protease inhibitor mixture (α-complete, Roche Molecular Biochemicals) and harvested by centrifugation. Pellets were frozen in liquid N_2 and stored at −80 °C until use. Frozen pellets were resuspended in 100 μl of 2× sample buffer and lysed by vigorous vortexing for 12 min with an equal volume of glass beads at 4 °C. After removal of glass beads, lysates were boiled for 5 min. Proteins were resolved by SDS-PAGE on a 7.5 or 12% gel for 2 h at 30 mA and analyzed by immunoblotting using either anti-Myc antibody (9E10, BAbCO) or anti-PSTAIRE antibody (this recognizes Cdc28 and Pho85; Santa Cruz Biotechnology). Preparation of cell lysates for analysis of Hog1 phosphorylation was as described (3), and phosphorylated Hog1–3HA was detected by anti-phospho-p38 antibody (Cell Signaling Technology) and Hog1–3HA was detected by anti-HA antibody (HA.11, BAbCO) as a loading control. For all immunoblots, horseradish peroxidase-conjugated second antibodies were used, and blots were visualized by ECL detection systems (Amersham Biosciences).

Hog1 Kinase Assay—Hog kinase assay in *PTC4* or *PTP2* overexpressed cells was performed as follows. A Hog1-HA integrated strain (SHI119) was transformed with vector only (YEp51) or pGAL-PTC4 (YEp51-PTC4). The cells were grown to 4 × 10^6 cells/ml in SR minus leucine medium at 28 °C and shifted to SG minus leucine medium and induced *PTC4* gene expression. After 1.5 h of induction, cells were exposed to 0.4 M KCl for various periods of time. Cells were harvested by centrifugation and lysed by vigorous vortexing for 12 min with an equal volume of glass beads at 4 °C in buffer A (50 mM Tris-HCl (pH 7.5), 50 mM NaCl, 5 mM EGTA, 5 mM $MgCl_2$, 0.1% Triton X-100, and 1 mM DTT, containing protein phosphatase inhibitors (50 mM β-glycerophosphate, 10 mM sodium vanadate, and 10 mM NaF) and protease inhibitors (1 mM PMSF and inhibitor mixture; Roche). The lysates were

clarified by centrifugation, 14,000 rpm for 20 min at 4 °C, and Hog1-HA was immunoprecipitated by incubation with 2 mg of total protein, 5 μl of anti-HA antibody (HA.11, 1 mg/ml), and 30 μl of protein A beads (Sigma) for 90 min at 4 °C. The immunoprecipitates were washed once with buffer A, twice with buffer B (50 mM Tris-HCl (pH 7.5), 150 mM NaCl, 5 mM EGTA, 5 mM $MgCl_2$, 1 mM DTT, 10 mM sodium vanadate, 10 mM NaF, and 1 mM PMSF), and once with kinase assay buffer (50 mM Tris-HCl (pH 7.5), 50 mM NaCl, 5 mM EGTA, 5 mM $MgCl_2$, 1 mM DTT, 1 mM sodium vanadate). The 25-μl supernatants of immunoprecipitates were used for immunoblotting as a loading control. To assay Hog1 kinase activity, Hog1-HA bound to protein A beads was incubated with [γ-^{32}P]ATP (5 μCi) and 45 μg of myelin basic protein (MBP, Sigma) for 30 min at 30 °C. Incorporation of ^{32}P into MBP was assessed by SDS-PAGE and quantified by BAS-1800 Bioimaging analyzer. In the experiments shown in Fig. 2, Δ*cnb1* Δ*mpk1* strain (TNP36) was transformed with vector only, pGAL-PTC4 (pNV7-PTC4), or pGAL-PTP2 (pSSP25, Ref. 3). The cells were grown to 6–8 × 10^6 cells/ml in SR minus uracil medium containing 1 M sorbitol at 28 °C and shifted to SG minus uracil medium without sorbitol. Hog1 protein was immunoprecipitated by anti-Hog1 antibody (y-215, Santa Cruz Biotechnology.) with protein A beads and assayed for kinase activity as described above.

Fluorescence-activated Cell Sorting Analysis, Fluorescence Staining, and Microscopy—Approximately 1 × 10^7 cells from yeast culture were harvested by centrifugation and resuspended in 300 μl of 0.2 M Tris-HCl (pH 7.5). Cells were fixed by addition of 700 μl of cold ethanol gradually with vortexing, followed by incubation for overnight at −20 °C. The fixed cells were washed with the same buffer containing RNase A (1 mg/ml) for 3 h at 30 °C. The cells were stained with 100 μl of propidium iodide (50 μg/ml) solution in 4 mM sodium citrate, 10 mM NaCl, and 0.1% Nonidet P-40 for 15 min on ice. The cells were analyzed by FACSCalibur (Becton Dickinson). F-actin was visualized by staining with rhodamine-conjugated phalloidin, as described (24). Quantification of cumulative percentage of bud formation and nuclear division during cell cycle progression in various strains that were synchronized with α-factor was determined by microscopic observation and propidium iodide staining. At least 300 cells were counted for each time point.

RESULTS

Identification of PTC4 cDNA as a High Dosage Suppressor of the Synthetic Lethality of the Δcnb1 Δmpk1 Double Deletion—To clarify the cellular event(s) that are regulated by the Ca^{2+} signaling pathways (calcineurin and Mpk1 mitogen-activated protein kinase cascade), we screened for the complementary DNA (cDNA), overexpression of which could rescue the synthetic lethality of the Δ*cnb1* Δ*mpk1* strain. Because the double deletion mutant can grow in the presence of an osmotic stabilizer (*e.g.* 1 M sorbitol), a yeast cDNA library constructed in an expression vector (pNV7) driven by the galactose-inducible *GAL1* promoter was introduced into the Δ*cnb1* Δ*mpk1* cells grown in the presence of sorbitol. The cells were spread on selection plates (SD minus uracil) containing sorbitol. From ~35,000 Ura^+ transformants, 85 transformants that could grow on YPG plate, but not on YPD plate (both plates without sorbitol), were selected. Six plasmids that reproducibly conferred viability to the Δ*cnb1* Δ*mpk1* strain on the YPG plate were recovered. The cDNA contained in the plasmids was designated *DSL* (for dose suppressor of lethality as a result of the Δ*cnb1* Δ*mpk1* double deletion). Nucleotide sequences of the inserts were determined. One of the isolates (*DSL1*) contained a *PTC4* cDNA, encoding a PP2C family protein phosphatase of unknown function (22).

The Lethality of the Δcnb1 Δmpk1 Strain Is Suppressed by the Additional Deletion of the HOG1 Gene—The PP2C family of protein phosphatases are commonly known as negative regulators of the MAPK cascade in various organisms, including the StyI/Spc1 pathway in *Schizosaccharomyces pombe*, and the p38 and c-Jun N-terminal kinase pathways in mammalian cells (25, 26). Likewise, the HOG pathway of *S. cerevisiae* is negatively regulated by the Ptc1, -2, and -3 PP2C family of phosphatases (3, 9). However, the physiological function of Ptc4 is not understood. We presumed that the phenotypic suppression might have been the result of the down-regulation of the HOG pathway by *PTC4* overexpression. If this were the case, the lethality of the Δ*cnb1* Δ*mpk1* strain should be suppressed by a defective HOG pathway. As expected, the Δ*cnb1* Δ*mpk1* Δ*hog1* triple deletion mutant was viable on YPD plates at 30 °C and even at 37 °C (Fig. 1*A*). In contrast, the Δ*cnb1* Δ*mpk1* double deletion had no significant effect on the osmosensitivity of the Δ*hog1* strain (Fig. 1*A*), suggesting that the Ca^{2+} signaling pathway and the HOG pathway are antagonistic in the growth regulation, but not in the high osmolarity response.

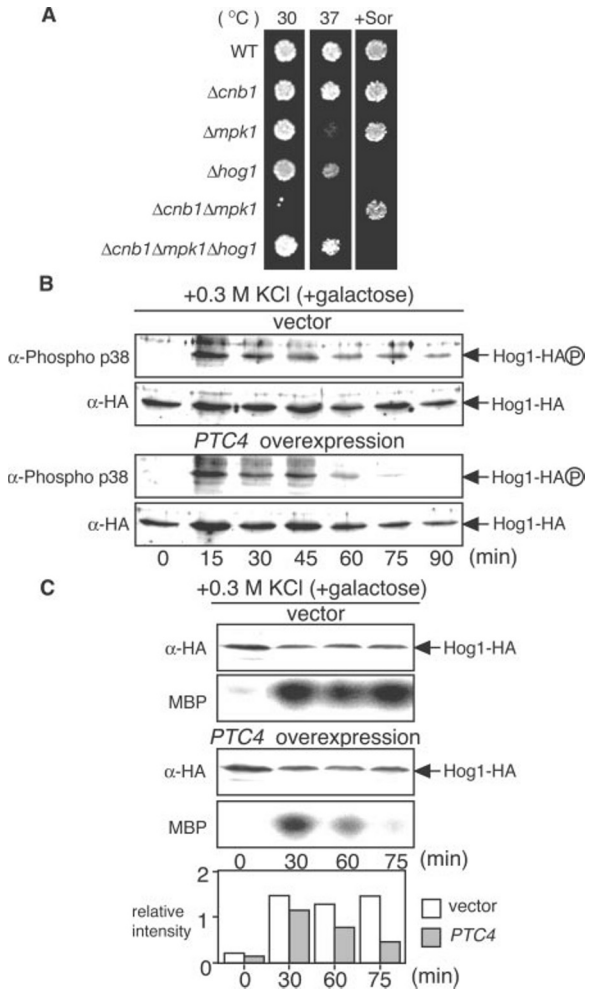

FIG. 1. ***PTC4* overexpression suppresses the lethality of the Δ*cnb1* Δ*mpk1* strain by negatively regulating Hog1 MAPK.** *A*, effect of *HOG1* deletion (Δ*hog1*) on the growth of Δ*cnb1* Δ*mpk1* strain. WT (W303), Δ*hog1* (SOS5), Δ*cnb1* (DHT14), Δ*mpk1* (TNP46), Δ*cnb1* Δ*mpk1* (TNP36), or Δ*hog1* Δ*cnb1* Δ*mpk1* (SOS48) cells were spotted on agar plates of YPD, or YPD + 1 M sorbitol (+*Sor*), and cultured for 2 days at the indicated temperature. *B*, effect of *PTC4* overexpression on the high osmolarity-induced Hog1 phosphorylation. WT (W303) cells transformed with YEp51 (vector) or YEp51-PTC4 (pGAL-PTC4) were grown in SR minus leucine (same composition as SD minus leucine, except 2% raffinose was used instead of dextrose) to early log phase and shifted to SG minus leucine to induce the *PTC4* gene expression and incubated for 1.5 h before exposure to 0.3 M KCl. Samples were taken at the indicated times. Whole-cell extracts were prepared, and immunoblotting was performed with anti-phospho-p38 or anti-HA as a loading control. *C*, Hog1 kinase activity was measured using the same cell extracts. Immunoprecipitated Hog1-HA was incubated with MBP and [γ-^{32}P]ATP. The level of Hog1-HA in lysate was assessed by immunoblotting with anti-HA antibody. The radiolabel incorporated into MBP was quantified by BAS1800 Bioimaging analyzer.

Hog1 activation is the result of the phosphorylation of both Thr-174 and Tyr-176. To examine whether the *PTC4* gene down-regulates Hog1, we compared the levels of Hog1 phosphorylation in the strains with or without overexpressing

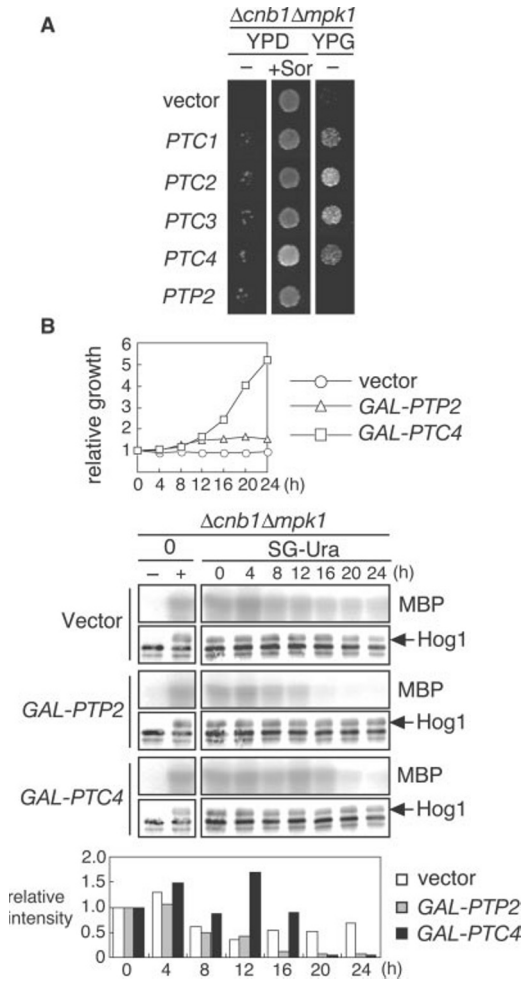

FIG. 2. **Effect of overexpression of the *PTC* and *PTP2* genes on the growth suppression of the lethality (*A*) and Hog1 kinase activity (*B*) of the Δ*cnb1* Δ*mpk1* strain.** *A*, the Δ*cnb1* Δ*mpk1* (TNP36) cells transformed with galactose-inducible plasmids bearing various PP2C genes (YEplac195GAL-PTC1, YEp112GAL-PTC2, YEplac112GAL-PTC3, pNV7-PTC4, and pSSP25) and empty vector containing an osmotic stabilizer (1 M sorbitol). The transformants were spotted on YPD, or YPD + 1 M sorbitol (+*Sor*) and YPG and cultured for 2 days at 30 °C. *B*, the Δ*cnb1* Δ*mpk1* (TNP36) cells transformed with galactose-inducible plasmids bearing *PTC4* or *PTP2* gene (pNV7-PTC4 and pSSP25) or empty vector were grown in SR minus uracil containing osmotic stabilizer (1 M sorbitol) to mid-log phase and shifted to SG minus uracil and induced gene expression. Samples were taken at the indicated times, and Hog1 kinase activity was measured (see "Materials and Methods"). The level of immunoprecipitated Hog1 was assessed by immunoblotting with anti-Hog1 antibody. The radiolabel incorporated into MBP was quantified by BAS1800 Bioimaging analyzer.

PTC4 gene from the *GAL1* promoter by using polyclonal antibody against phospho-p38, which cross-reacts with phospho-Hog1. As expected, the level of the high osmolarity-induced Hog1 phosphorylation was significantly reduced by *PTC4* overexpression (Fig. 1*B*). This result was further verified by measuring the Hog1 kinase activity using [γ^{32}-P]ATP and MBP as a substrate. Indeed, the kinase activity was reduced by *PTC4* overexpression (Fig. 1*C*). To see whether the suppression of this lethality is the result of the inhibition of the HOG pathway, we examined whether the overexpression of other negative regulators (*PTC1*, *-2*, and *-3* and *PTP2*) known for the HOG pathway can suppress the lethality of the Δ*cnb1* Δ*mpk1* strain. Overexpression of the *PTC1*, *-2*, or *-3* gene could suppress the lethality to a degree similar to the overexpression of the *PTC4* gene (Fig. 2*A*). However, overexpression of the *PTP2* gene failed to suppress the lethality (Fig. 2*A*). We next examined whether overexpression of *PTC4* or *PTP2* gene truly reduced the Hog1 kinase activity in the Δ*cnb1* Δ*mpk1* strain. As the result, overexpression of these genes reduced the basal level activity of Hog1 kinase in the Δ*cnb1* Δ*mpk1* strain (Fig. 2*B*). The *PTP2* overexpression inhibited the Hog1 activity, but it could not suppress the growth defect (Fig. 2*B*). For the difference in the effect of the overexpression of these genes on the growth of the Δ*cnb1* Δ*mpk1* strain, see "Discussion."

Δ*hog1 Mutant Displays Ca^{2+}-induced G_2 Delay and Polarized Bud Growth*—Deletion of the HOG pathway has been shown to partially suppress the defect of the mutants in cell wall integrity signaling in a manner mediated by the SVG (STE vegetative growth) pathway that regulates the cell wall integrity in parallel with the Mpk1 MAPK pathway (27). In this process, the HOG pathway seemed to negatively regulate cell wall integrity through the SVG pathway, antagonizing the Mpk1 MAPK pathway. Supporting this possibility, it was shown that the defect of the HOG pathway causes an activation of the STE pathway (28), which in turn may lead to the activation of cell wall integrity.

The HOG pathway seems to be also involved in G_2/M cell-cycle regulation. Deletion of *HSL1* gene, which encodes a negative regulator of Swe1 kinase, suppressed the lethality caused by the double deletions of the *CNB1* and *MPK1* genes, suggesting that the HOG pathway and the Ca^{2+} signaling pathways also antagonize in G_2/M cell-cycle progression (data not shown). In the Ca^{2+}-triggered, Swe1-mediated G_2/M cell-cycle regulatory mechanism, Zds1 inhibits *SWE1* transcription in G_2 phase, antagonizing the Ca^{2+} signaling pathways (21. 29). Therefore, the Δ*zds1* strain exhibits various Ca^{2+} phenotypes, including hypersensitivity to $CaCl_2$ (>50 mM), G_2 cell-cycle delay, and polarized bud growth. If the HOG pathway and the Ca^{2+} signaling pathways antagonize one another in cell-cycle regulation, it would be expected that the Δ*hog1* strain growing in the presence of $CaCl_2$ would display a phenotype analogous to that of the Δ*zds1* strain. This was indeed the case. The Δ*hog1* strain exhibited the Ca^{2+} phenotypes similar to those of the Δ*zds1* strain (Fig. 3, *A* and *B*). The similar phenotypes were not observed with the Δ*hog1* strain by sorbitol or other cations (*e.g.* Mg^{2+} and Na^{+}), suggesting that the Ca^{2+} phenotypes exhibited by the Δ*hog1* strain were distinct from those of the high osmolarity of the solutes (Fig. 3*A* and data not shown).

The Ca^{2+} phenotypes of the Δ*zds1* strain were shown earlier to be suppressed by the deletion of the *CNB1*, *MPK1*, or *SWE1* gene (21). So we asked whether calcineurin, Mpk1, or Swe1 is required for the phenotype displayed by the Δ*hog1* strain. The effects of $CaCl_2$ on the Δ*hog1* strain were all rescued by the deletion of *CNB1* or *SWE1*, but not that of *MPK1* (Fig. 3, *A* and *B*). However, because the effect of the *SWE1* deletion was only partial, it was suggested that the HOG pathway has additional target(s) in the Ca^{2+}-mediated growth regulation.

Swe1 Degradation in the Δhog1 Strain Is Delayed by Ca^{2+}—The *SWE1* mRNA level of WT cells fluctuates during the cell cycle, peaking in G_1/S and declining just before the onset of mitosis (21, 29). We first examined whether the HOG pathway is involved in the transcriptional regulation of the *SWE1* gene by measuring the *SWE1* mRNA levels in the presence or absence of 50 mM $CaCl_2$ in a synchronized cell cultures by α-factor. The fluctuation pattern was not dependent on the presence of the *HOG1* gene, indicating that Hog1 is not important for the transcriptional regulation of the *SWE1* gene (data not shown).

We next examined whether the HOG pathway is involved in post-transcriptional Swe1 regulation. The accumulation of Swe1 is periodic during the cell cycle, peaking at the time of bud emergence and declining before nuclear division (30, 31). We constructed various strains (WT, Δ*cnb1*, Δ*hog1*, and Δ*hog1* Δ*cnb1*, each on the Δ*swe1* background) expressing a Myc

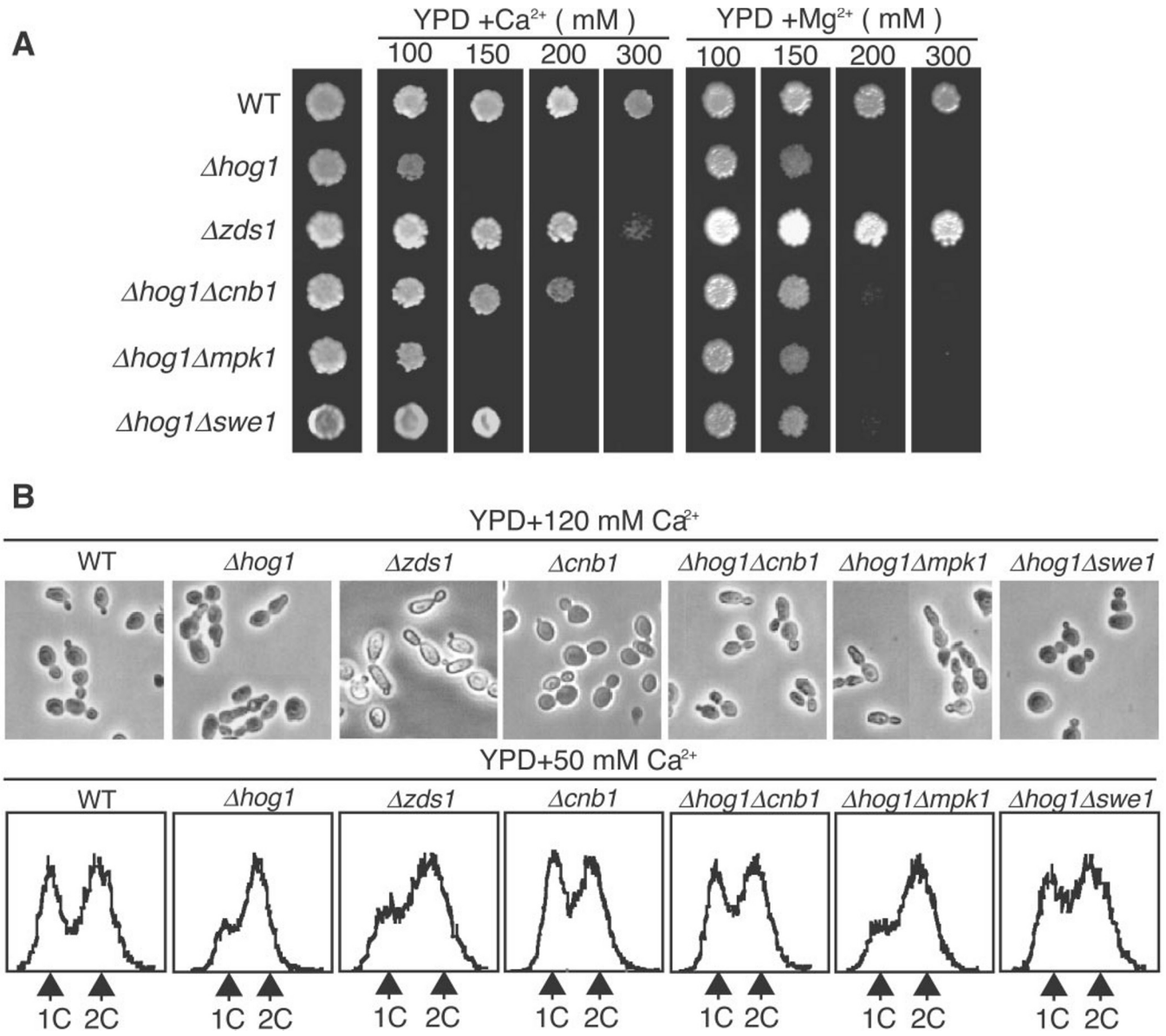

FIG. 3. **Ca^{2+} phenotypes of Δ*hog1* strain are suppressed by Δ*cnb1*, or Δ*swe1*, but not Δ*mpk1*.** *A*, growth of various strains on solid medium, containing various concentrations of $CaCl_2$, or $MgCl_2$. WT (W303), Δ*hog1* (SOS5), Δ*zds1* (YAT1), Δ*hog1* Δ*mpk1* (SOS27), Δ*hog1* Δ*swe1* (SOS44), or Δ*hog1* Δ*cnb1* (SOS31) cells were spotted on YPD plates added with the indicated concentrations of $CaCl_2$, or $MgCl_2$ and incubated for 2 days at 28 °C. *B*, cell morphology and fluorescence-activated cell sorting analysis of various strains after 6 h of incubation at 28 °C in YPD medium added with the indicated concentration of $CaCl_2$.

epitope-tagged Swe1 from the chromosomally integrated gene and compared the fluctuation patterns of Myc-tagged Swe1 by immunoblot analysis in synchronized cell cultures. The Myc-Swe1 construct was fully functional *in vivo* (data not shown). The G_1 cells synchronized with α-factor were released into YPD medium with or without 50 mM $CaCl_2$. The cell-cycle progression in synchronous cell cultures was monitored by the determination of nuclear division and DNA contents (Fig. 4, *B* and *C*). As previously reported (30, 31), the Swe1 level of the WT strain fluctuated during the cell cycle. The slower migrating species of Swe1 represent a phosphorylated isoform, and the phosphorylation occurs prior to its degradation coincidental with the onset of mitosis (31). Immediately after the degradation, the faster migrating species of Swe1 re-appeared. In YPD medium, there was no significant difference among the strains in the periodic patterns of the Swe1 level and the timing of nuclear division. However, in the Δ*hog1* cells cultivated with $CaCl_2$, the Swe1 level was sustained for 30 min longer, and correspondingly, the onset of mitosis was delayed by 30 min, in comparison with those in WT cells treated similarly. This result suggests that Ca^{2+} caused a delay in Swe1 degradation in the Δ*hog1* strain. Both Ca^{2+}-induced Swe1 stabilization and the delay of nuclear division in the Δ*hog1* strain were shortened to 15 min by *CNB1* deletion, indicating that the Swe1 stability is antagonistically regulated in a manner mediated by the HOG pathway and calcineurin (compare Δ*hog1* and Δ*hog1* Δ*cnb1* strains in Fig. 4*A*).

The HOG Pathway Promotes Bud Emergence, whereas Calcineurin Inhibits Actin Polarization—Using the same synchronous cell cultures described in the previous section, we also determined the time course of bud emergence (Fig. 4*B*). In YPD medium, no significant difference was observed among the strains in the timing of bud emergence. In the presence of 50 mM $CaCl_2$, bud emergence in the Δ*hog1* strain was delayed by 30 min compared with that in the WT strain. In the presence of sorbitol, the Δ*hog1* strain showed a delay of bud emergence by 15 min compared with that of the WT strain. The Ca^{2+}-induced delay in the Δ*cnb1* strain was shortened to 15 min (compare

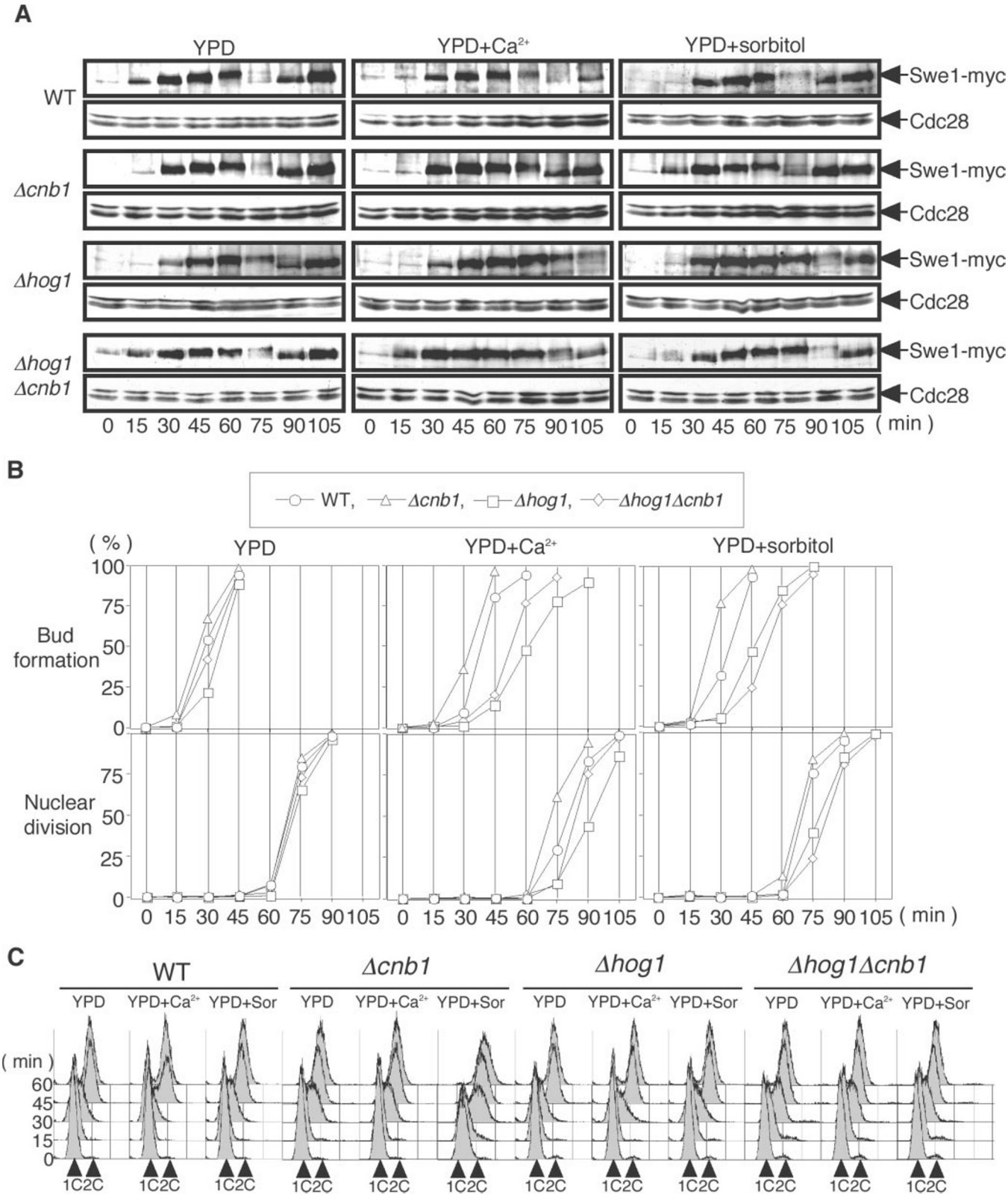

FIG. 4. **Effects of $CaCl_2$ on the Swe1 accumulation, nuclear division, bud formation, and DNA content in synchronized cell culture of various strains.** *A*, the fluctuation of the Swe1 abundance during the cell cycle in the cells synchronized with α-factor. WT (SHI26), Δ*cnb1* (SHI63), Δ*hog1* (SHI27), or Δ*hog1* Δ*cnb1* (SHI30) strains were grown in YPD to early-log phase, and the cells were then synchronized as described under "Materials and Methods." Whole-cell extracts were prepared and analyzed by immunoblotting with an antibody against Myc-Swe1 and one against Cdc28 as a loading control. *B*, quantification of cumulative percentage of nuclear division and bud formation during cell-cycle progression in various strains in the cell cultures prepared as in *A* was determined by microscopic observation following PI staining; at least 300 cells were counted for each time point. The cells were released into YPD medium with or without 50 mM $CaCl_2$ (+*Ca*$^{2+}$) or 150 mM sorbitol (+*Sor*). Samples were taken at an interval of 15 min after removing the α-factor. *C*, DNA content of various strains in a synchronized culture prepared as in *A* after release from arrest in G_1.

Δ*hog1* and Δ*hog1* Δ*cnb1* in Fig. 4*B*). In contrast, the sorbitol-induced delay was not altered in the Δ*cnb1* strain (Fig. 4*B*). Moreover, no significant delay was observed in DNA replication of various strains in the presence of 50 mM $CaCl_2$, indicating that the Ca^{2+}-induced delay of bud formation is not simply a reflection of the decelerated cell cycle by Ca^{2+} (Fig. 4*C*). Taken together, these results indicated that bud emergence is antagonistically regulated, positively by the HOG pathway and negatively by calcineurin.

To address whether Ca^{2+}, rather than the osmotic stress, is specifically responsible for the severe delay in mitosis caused by $CaCl_2$, we examined whether osmotic stress of sorbitol might induce a similar effect. In YPD medium containing 150 mM sorbitol, which gives an osmolarity equivalent to that of 50 mM $CaCl_2$, both Swe1 degradation and the nuclear division of the Δ*hog1* cells were delayed by 15 min compared with those of WT cells. This delay was shorter than that caused by $CaCl_2$ (30 min; Fig. 4, *A* and *B*). Moreover, the delays in Swe1 degradation and cell-cycle progression caused by sorbitol were not alleviated by the deletion of calcineurin, suggesting that the mechanisms underlying the delays were different for Ca^{2+} and sorbitol (Fig. 4, *A* and *B*).

To further clarify the roles of these pathways in the control of bud emergence, we examined the effects of $CaCl_2$ on bud emergence and actin polarization at the bud site in α-factor-synchronized cells (Fig. 5). Actin polarization was determined by rhodamine-phalloidin staining. No significant difference was observed in the kinetics of actin polarization among the strains (WT, Δ*cnb1*, Δ*hog1*, and Δ*hog1* Δ*cnb1*) after release of the cells to YPD medium. The timing of actin polarization of WT and the Δ*hog1* cells was only slightly delayed after release to the medium containing 50 mM $CaCl_2$ (compare $\pm Ca^{2+}$ at 15 min for WT and Δ*hog1* cells). However, bud emergence of the Δ*hog1* cells was delayed from that of WT cells by 30 min (compare WT and Δ*hog1* cells, $+Ca^{2+}$ at 45–60 min), although the actin patches were localized apparently normally at the presumptive bud site. The delay in actin polarization was nearly completely abolished in the Δ*cnb1* cells, although bud emergence was still delayed by 15 min (compare WT and Δ*hog1* cells, $+Ca^{2+}$ at 15–30 min). The Ca^{2+}-induced delay of bud emergence in the Δ*hog1* strain was only partially suppressed by the deletion of calcineurin (compare Δ*hog1* and Δ*hog1* Δ*cnb1* cells, $+Ca^{2+}$ at 45 min).

Calcineurin is known to regulate cellular Ca^{2+} homeostasis. Defect of calcineurin leads to increase Ca^{2+} tolerance by increasing vacuolar sequestration of Ca^{2+} from the cytosol (32, 33). Therefore, the effect of Δ*cnb1* on actin polarization could be the result of an alteration of cellular Ca^{2+} homeostasis. We investigated whether calcineurin truly regulates actin polarization by using a constitutively active form of calcineurin, containing the C-terminal truncated form of catalytic subunit (*CMP2ΔC*). The galactose-inducible *GAL1-CMP2ΔC* construct was introduced to the *URA3* locus of WT strain and an experiment similar to that described above was performed without addition of $CaCl_2$. Overexpression of *CMP2ΔC* inhibited actin polarization to the bud site (Fig. 6, compare *+glucose (off)* and *+galactose (on)*). The overexpression of *CMP2ΔC* did not lead to a delay in the progression of DNA replication (Fig. 6*B*) consistently with the results obtained with the addition of Ca^{2+} (Fig. 4*C*). These results indicated that the HOG pathway promotes bud emergence after actin polarization, whereas calcineurin inhibits actin polarization (see "Discussion").

The Calcineurin-Crz1/Tcn1 Pathway Is Required for the Down-regulation of the HOG Pathway—To further investigate the antagonizing mechanism between the 2 pathways, we examined whether calcineurin down-regulates the HOG pathway by determination of phospho-Hog1 with anti-phospho-p38 antibody. In WT cells, the Hog1 phosphorylation induced by $CaCl_2$ was transient, peaking at 15 min and disappearing by 30 min of the treatments (Fig. 7*A*). In the Δ*cnb1* strain, Hog1 phosphorylation was induced by $CaCl_2$ similarly as in WT strain, but the phosphorylation level increased to a much higher level and sustained longer than in the WT one (Fig. 7*A*).

We further examined whether Crz1/Tcn1, a transcription factor activated by calcineurin, was involved in this process (17, 18). The level of Ca^{2+}-induced Hog1 phosphorylation in the Δ*crz1* strain was similarly high as that in the Δ*cnb1* strain (Fig. 7*A*). Moreover, Δ*crz1* and Δ*cnb1* mutations did not exhibit an additive effect on the level of Hog1 phosphorylation, suggesting that calcineurin and Crz1 regulate Hog1 phosphorylation in a common pathway (data not shown). The Ca^{2+}-induced Hog1 hyperphosphorylation in the Δ*crz1* strain led to an increased expression level of *GPD1* mRNA compared with that in the WT strain, suggesting that the negative regulation of the HOG pathway was mediated by the Crz1 transcription factor (data not shown). We next examined the possibility that various protein phosphatase(s) known to inhibit the HOG pathway are involved in the regulation of Hog1 by Crz1. We examined by Northern blot analysis the effect of $CaCl_2$ in WT cells on the mRNA levels of various phosphatases, which included the PP2C family phosphatases (Ptc1, -2, -3, and -4) and the protein-tyrosine phosphatases (Ptp2 and -3). Of the mRNA levels of these phosphatase genes, only that of *PTP2* gene was moderately decreased by the deletion of *CRZ1* gene (data not shown). However, the calcineurin-Crz1 pathway-dependent regulation of *PTP2* transcription seemed inadequate to explain the Hog1 hyperphosphorylation induced by Ca^{2+}. The activation of the HOG pathway in response to high osmolarity is mediated by two upstream branches, one through the Sho1 sensor and the other through the two-component system consisting of Sln1, Ypd1, and Ssk1 (2–6). To address which of the two branches is responsible for the inhibition of Hog1 by Ca^{2+}, we compared the Ca^{2+}-induced Hog1 phosphorylation levels among the strains deleted for a component of the HOG pathway, together with the regulatory subunit of calcineurin (*i.e.* Δ*cnb1* Δ*pbs2*, Δ*cnb1* Δ*ste11*, and Δ*cnb1* Δ*ssk1* strains) (Fig. 7*A*). Hog1 phosphorylation was not detectable in the Δ*cnb1* Δ*pbs2* strain, indicating that $CaCl_2$ activates Hog1 through Pbs2 (Fig. 7*A*). The Ca^{2+}-induced Hog1 hyperphosphorylation was observed in the Δ*cnb1* Δ*ste11* strain, but not in the Δ*cnb1* Δ*ssk1* strain, suggesting that the calcineurin-Crz1 pathway inhibits the Sln1, but not Sho1, branch, of the HOG pathway. Moreover, the enhancement of Hog1 phosphorylation in Δ*cnb1* strain was also observed by sorbitol (300 mM) that causes an osmolarity equivalent to that of 100 mM $CaCl_2$ (Fig. 7*B*). It was recently shown that a transient increase in the cytosolic Ca^{2+} is induced from the vacuolar stores by hyper-osmotic stress (34). The calcineurin-Crz1 pathway is important in the regulation of intracellular Ca^{2+} homeostasis. Therefore, these results suggested that the increase in cytosolic Ca^{2+} may down-regulate the HOG pathway through the regulation of the Sln1 branch (see "Discussion").

DISCUSSION

HOG Pathway and Calcineurin Antagonize in Growth Regulation—We have shown here that the *HOG1* deletion remarkably suppressed the lethality caused by the simultaneous loss of calcineurin and the Mpk1 MAPK pathway. Thus, the Δ*cnb1* Δ*mpk1* Δ*hog1* triple disruption mutant grew apparently normally on YPD plate at 30 °C and even at 37 °C, a restrictive temperature for the Δ*mpk1* strain. The lethality of the Δ*cnb1* Δ*mpk1* strain is attributable mainly to a defect in the cell wall construction for the following reasons. 1) The lethality is rem-

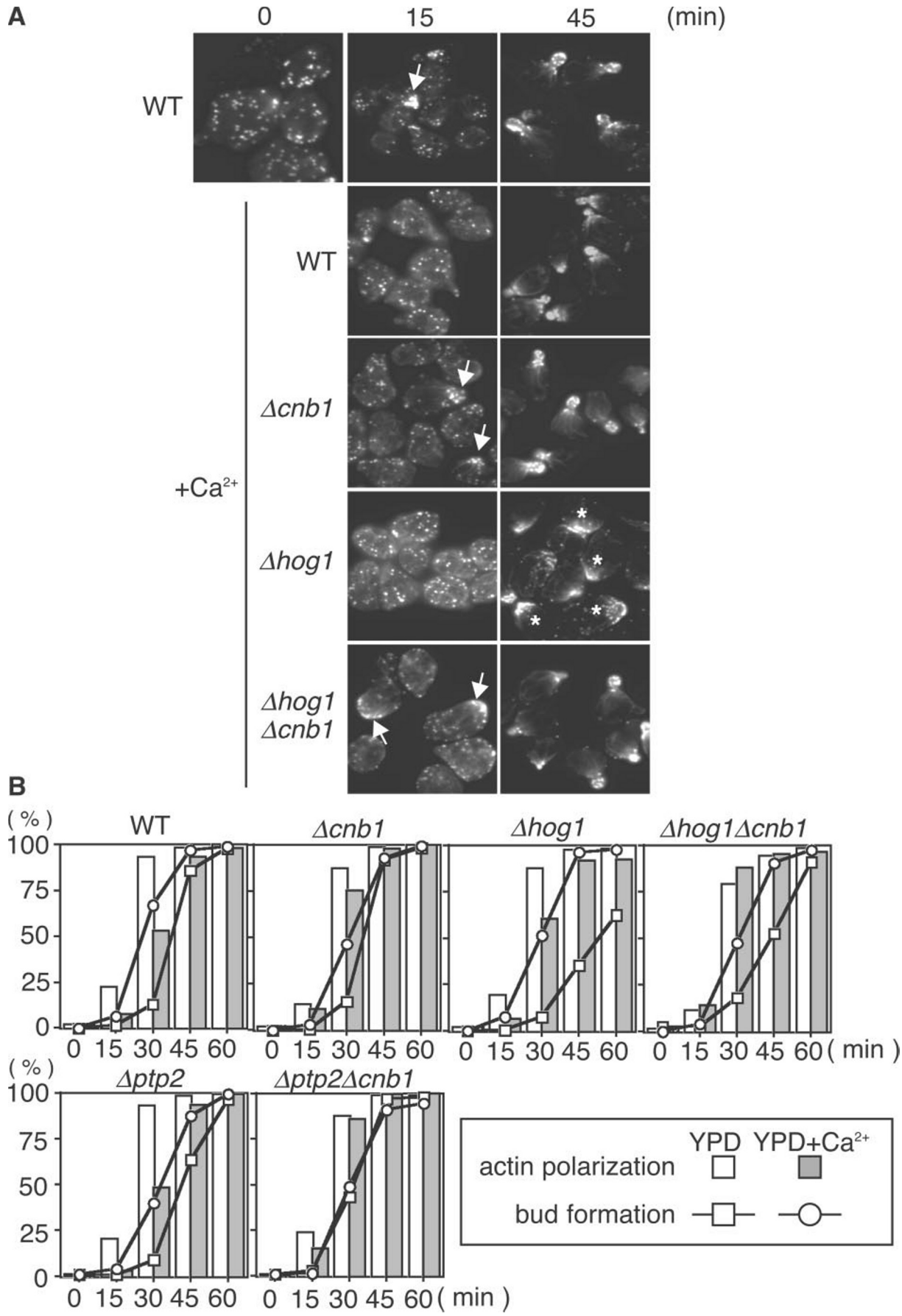

FIG. 5. **Calcineurin negatively regulates actin polarization and bud emergence, whereas Hog1 positively regulates bud formation after actin polarization.** WT (W303), Δ*cnb1* (DHT14), Δ*hog1* (SOS5), or Δ*hog1* Δ*cnb1* (SOS31), Δ*ptp2* (SH7687), or Δ*ptp2* Δ*cnb1* (SHI334) was grown in YPD medium to early-log phase, and cells were synchronized as described under "Materials and Methods." The cells were released into

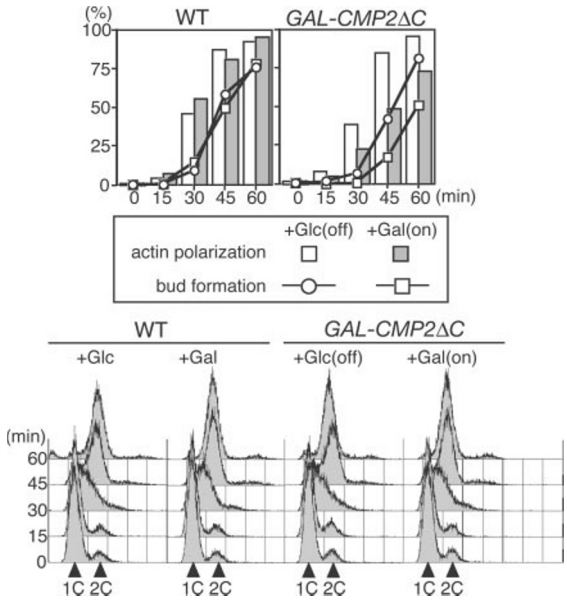

FIG. 6. **Overexpression of constitutively active calcineurin inhibits the actin polarization to the bud site.** *A*, WT (W303) strain and *GAL-CMP2ΔC* integrating strain (SHI290) was grown in YPR to early-log phase, and cells were synchronized as described under "Materials and Methods." The cells were released into YPD or YPG medium. Samples were taken at an interval of 15 min after removing the α-factor, and cells were fixed with formaldehyde. The actin polarization and the bud formation of the cells were monitored by microscopic observation with rhodamine-phalloidin staining. The results were quantified and plotted as time after release *versus* percentage of actin patches localized at the incipient bud site (*solid column*) and bud formation (*line*); at least 300 cells were counted for each time point. *White bars* and *circular symbols*, in YPD medium. *Light gray bars* and *square symbols*, in YPG medium. *B*, DNA content of various strains in a synchronized culture prepared as in *A* after release from arrest in G_1.

edied by osmotic stabilizers added to the medium (20). 2) The expression of the *FKS2* gene, which encodes a glucan synthetase, is activated by the calcineurin-Crz1 pathway (35). 3) The Mpk1 MAPK cascade has been implicated in the expression of various genes involved in cell wall synthesis (1). The observation that the triple disruption mutant was viable on YPD plates even at 37 °C indicates that the HOG pathway negatively regulates the cell wall construction, antagonizing the Ca^{2+} signaling pathways.

Besides the cell wall, calcineurin and the Mpk1 pathway coordinately regulate the G_2/M cell-cycle progression through the regulation of Swe1 (21). Because the suppression of the synthetic lethality by the *HOG1* deletion was very potent, the HOG pathway and the Ca^{2+} signaling pathways were thought to counteract each other in diverse events of growth regulation, including cell wall synthesis and cell-cycle progression. In fact, the synthetic lethality was partially suppressed by the deletion of the Nim1-like kinase Hsl1, the negative regulatory kinase of Swe1 (data not shown). The involvement of the HOG pathway in cell-cycle regulation was further supported by the observations that the HOG pathway regulates stability of Swe1 (Fig. 3*A*) and the effect of *HOG1* deletion was partially suppressed by the *SWE1* deletion (data not shown).

The Δ*cnb1* Δ*mpk1* synthetic lethality was suppressed by overexpression of *PTC1*, -2, *-3*, or *-4*, encoding the serine/threonine phosphatase PP2C family known as the negative regulator of the HOG pathway, supporting the notion that the HOG pathway and the Ca^{2+} signaling pathways antagonize each other in growth regulation. However, overexpression of the tyrosine phosphatase Ptp2 failed to suppress the lethality. This result suggests that the PP2C overexpression suppressed the growth of the Δ*cnb1* Δ*mpk1* strain by dephosphorylating a target protein phosphorylated by the serine/threonine kinase Hog1. Further investigation is necessary to elucidate the mechanism of the lethality.

Calcineurin and the HOG Pathway Regulate Distinct Processes of Bud Emergence—The HOG pathway and calcineurin/Mpk1 MAPK pathways perform antagonistic roles in the regulation of bud emergence. The detailed analysis of the kinetics of the bud emergence and the actin localization in synchronized cell cultures revealed that calcineurin and the HOG pathway regulate distinct processes of bud emergence (Fig. 5). In the WT strain, the actin polarization at the presumptive bud site and bud emergence were shortly delayed (~15 min) by Ca^{2+}. The delays were abrogated in the Δ*cnb1* strain, indicating that the delays occurred in a calcineurin-dependent manner. Compared with the wild-type strain, the delay in bud emergence induced by Ca^{2+} in the Δ*hog1* strain was longer. Although bud emergence in the Δ*hog1* strain was severely delayed by Ca^{2+}, actin polarization was only slightly affected. These results indicated that the Hog1 activation stimulated bud emergence at a step after actin had correctly become localized at the bud site. The Ca^{2+}-induced delay of bud emergence in the Δ*hog1* strain was only partially suppressed by the deletion of calcineurin, suggesting that the *CNB1* deletion can suppress the defect in actin polarization, but not the bud emergence. Taken together, these results indicated that the processes of the bud emergence that are regulated by calcineurin and the HOG pathway are distinct. Calcineurin inhibits actin polarization, an early step of bud emergence, whereas Hog1 promotes bud emergence at a step after actin has become polarized. The identification of the targets of calcineurin in regulating actin polarization and that of the HOG pathway in bud emergence still remains to be made.

The G_2 delay caused by 50 mM $CaCl_2$ in Δ*hog1* strain may have been the result of the activation of the morphogenesis checkpoint. Supporting this notion, bud formation in the Δ*hog1* strain was severely delayed, although DNA replication was not significantly affected by $CaCl_2$ (Fig. 4, *B* and *C*). The morphogenesis checkpoint monitors abnormal bud formation and is functional in late G_1 to S phases, but is nonfunctional once the bud has grown to a critical size (31). It is possible that the defect of bud emergence caused by deregulated synthesis of the cell wall and the inhibition of the actin polarization in the Δ*hog1* may activate the morphogenesis checkpoint. Why did the Δ*hog1* strain exhibit a severe defect in bud emergence in the presence of Ca^{2+}? As a yeast cell buds, the cell wall must expand to fit the expanding plasma membrane. During expansion of the rigid cell wall, it must be weakened at the point of new growth to add newly made cell wall material. The severe defect in bud emergence in the Δ*hog1* cells would be explained by the deregulated synthesis of the cell wall at the bud site by the hyperactivation of the cell wall synthesis as a result of the absence of its negative regulator (Hog1) and by the activation of the Ca^{2+} signaling pathways. Alternatively, it is also possible that the delay in bud emergence might have resulted from the

YPD medium with or without 50 mM $CaCl_2$ (+Ca^{2+}). Samples were taken at an interval of 15 min after removing α-factor and fixed with formaldehyde. *A*, actin staining with rhodamine-phalloidin. The *arrowheads* indicate polarized actin at the incipient bud site, and the *asterisks* indicate defective bud emergence in Δ*hog1* cells. *B*, the results were quantified and plotted as time after release *versus* percentage of actin patches localized at the incipient bud site (*solid column*) and bud formation (*line*); at least 300 cells were counted for each time point. *White bars* and *circular symbols*, in YPD medium. *Light gray bars* and *square symbols*, in YPD plus 50 mM $CaCl_2$.

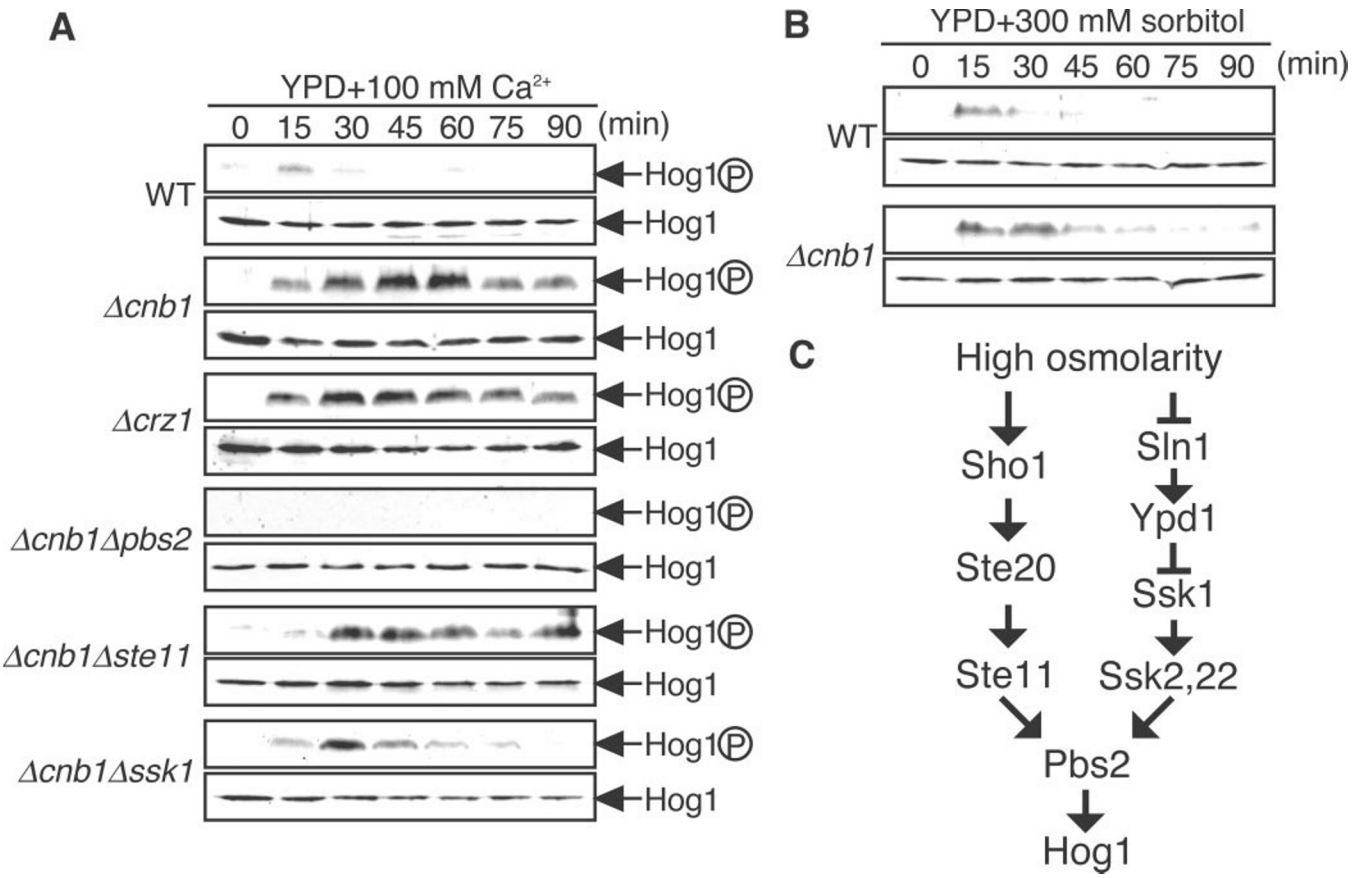

FIG. 7. **The calcineurin-Crz1 pathway required for the down-regulation of HOG pathway.** *A*, the effect of deletion of *CNB1*, *CRZ1/TCN1*, *PBS2*, *STE11*, or *SSK1* deletion on the Ca^{2+}-induced hyperphosphorylation of Hog1. WT (SHI119), Δ*cnb1* (SHI121), Δ*crz1* (SHI288), Δ*cnb1* Δ*pbs2* (SHI318), Δ*cnb1* Δ*ste11* (SHI131), or Δ*cnb1* Δ*ssk1* (SHI313) was grown in YPD medium to early-log phase, and the cells were then exposed to 100 mM $CaCl_2$ (+Ca^{2+}). Samples were taken at an interval of 15 min after addition of $CaCl_2$. Whole-cell extracts were prepared and immunoblotted with an antibody against phospho-p38 and with one against HA as a loading control. *B*, the effect of sorbitol on Hog1 phosphorylation in Δ*cnb1* strain. WT (SHI119) or Δ*cnb1* (SHI121) strain was grown in YPD medium to early-log phase, and the cells were then exposed to 300 mM sorbitol. Immunoblotting was performed as described in *A*. *C*, outline of the upstream branches of HOG pathway.

defect in recovery from the inhibition of protein synthesis. It was recently reported that the Δ*hog1* mutant was defective in the recovery from hypertonic stress-induced inhibition of protein synthesis (36).

It was suggested that Ca^{2+} signal inhibited bud emergence through inhibition of Hog1 in a manner mediated by the calcineurin-Crz1 pathway and through inhibition of actin polarization by calcineurin. If so, the inhibitory effect of Ca^{2+} on bud emergence would be abolished by the activation of Hog1. This was indeed the case. The delay in bud emergence that was still seen in the Δ*cnb1* strain was apparently totally abolished by the deletion of the *PTP2* gene (Fig. 5*B*).

We showed here that calcineurin was involved in the inhibition of actin polarization at the bud site. In the pathogenic fungus *Cryptococcus neoformans*, it was earlier suggested that calcineurin was required for the polar cell growth in mating and haploid fruiting (37). In the nerve cells, calcineurin was implicated in cell polarization (38).

The Ca^{2+}-induced inhibition of actin polarization in Δ*hog1* strain was not suppressed by the deletion of *CRZ1* (data not shown), suggesting that other target molecule(s) are involved in the regulation of actin polarization by calcineurin.

Cross-talk between the HOG Pathway and Ca^{2+} Signaling Pathway—Because the HOG pathway and the Ca^{2+} signaling pathways are regulated opposingly by high and low external osmolarity, respectively, the question arises as to whether these pathways regulate each other. Our data suggested that the calcineruin-Crz1 pathway was involved in the down-regulation of the HOG pathway through the regulation of the Sln1, but not Sho1, branch (Fig. 7*A*; see a model in Fig. 8). Further, Hog1 phosphorylation was sustained with the Δ*ste11* Δ*cnb1* strain, but not with the Δ*ssk1* Δ*cnb1* strain, suggesting that the calcienrin-Crz1 pathway is involved in the inhibition of the Sln1 pathway. The phosphorylation level of Hog1 in the Δ*ssk1* Δ*cnb1* strain decreased after 45 min of its activation, suggesting that the down-regulation of the Sln1 branch by the cal-

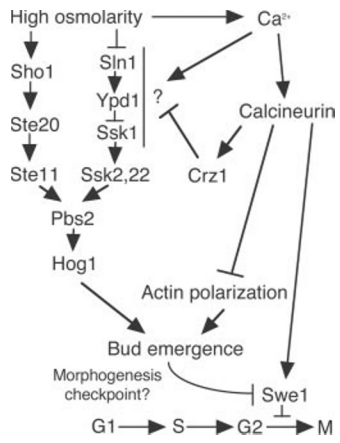

FIG. 8. **A schematic model to illustrate the antagonistic regulation of bud formation and the onset of mitosis by the HOG pathway and the Ca^{2+}-signaling pathways in budding yeast.**

cineurin-Crz1 pathway is important in the cross-talk regulation of the HOG pathway (Fig. 7*A*). The Hog1 phosphorylation in the Δ*cnb1* strain induced by 100 mM Ca^{2+} was significantly higher and sustained longer than that by 300 mM sorbitol, suggesting that Ca^{2+} is more potent than sorbitol in Hog1 activation (compare the phosphorylation levels of "Δ*cnb1*" samples in Fig. 7, *A* and *B*). Because hyperosmotic stress induces a transient increase in cytosolic Ca^{2+} from vacuolar stores (34), the difference in the effect of $CaCl_2$ and sorbitol on Hog1 phosphorylation may simply reflect the difference in the effect of exogenous $CaCl_2$ and hyperosmotic stress on the elevation of intracellular Ca^{2+}. How does Ca^{2+} activate the Sln1 branch of the HOG pathway? As previously suggested, the osmo-activated Sln1-Ypd1-Ssk1 phosphorelay system may be under a negative feedback regulation by accepting a phosphate group from glycerol 3-phosphate or related metabolic intermediate donors, which may be overproduced by glycerol-3-phosphate dehydrogenase, a target of the HOG pathway (5). The loss of calcineurin activity leads to elevation of the cytosolic Ca^{2+} concentration (32, 39, 40). If such a feedback regulatory mechanism that is mediated by a phosphorylated metabolite does exist for the HOG pathway, the elevation of intracellular Ca^{2+} may cause the formation of an insoluble complex with the phosphate compound, interfering with re-phosphorylation of the two-component system. Alternatively, it is possible that unknown Crz1 target genes are involved in this process. The mechanism by which the calcineurin-Crz1 pathway regulates the Sln1 branch still remains to be seen. Our observations provide evidence for a cross-talk between the Ca^{2+} signaling pathway and the HOG pathway. The activation of the p38 MAPK cascade by Ca^{2+} signal was recently reported with the p38 MAPK cascade of *Caenorhabditis elegans* (41). In mammalian cells, the p38 MAPK pathway is inhibited by calcineurin in a manner mediated by the transcriptional up-regulation of MAPK phosphatase-1 (42). It is possible that regulation of the p38 family MAPK pathway by the Ca^{2+} signaling pathways is conserved from yeast to higher eukaryotes.

On the basis of these data, we propose a model for the regulation of cell growth by the HOG pathway and calcineurin (Fig. 8).

Acknowledgments—We thank Kunihiro Matsumoto for the yeast cDNA library; Satoshi Harashima and Masaki Mizunuma for mutant strains, and Rinji Akada, Robert Booher, Tatsuya Maeda, and Mark Solomon for plasmids. We thank Masaki Mizunuma for helpful discussion.

REFERENCES

1. Gustin, M. C., Albertyn, J., Alexander, M., and Davenport, K. (1998) Mol. *Biol. Rev.* **62,** 1264–1300
2. Brewster, J. L., de Valoir, T., Dwyer, N. D., Winter, E., and Gustin, M. C. (1993) *Science* **259,** 1760–1763
3. Maeda, T., Wurgler-Murphy, S. M., and Saito, H. (1994) *Nature* **369,** 242–245
4. Maeda, T., Takekawa, M., and Saito, H. (1995) *Science* **269,** 554–558
5. Posas, F., Wurgler-Murphy, S. M., Maeda, T., Witten, E. A., Thai, T. C., and Saito, H. (1996) *Cell* **86,** 865–875
6. Posas, F., and Saito, H. (1998) *EMBO J.* **17,** 1385–1394
7. Jacoby, T., Flanagan, H., Faykin, A., Seto, A. G., Mattison, C., and Ota, I. (1997) *J. Biol. Chem.* **272,** 17749–17755
8. Wurgler-Murphy, S. M., Maeda, T., Witten, E. A., and Saito, H. (1997) *Mol. Cell Biol.* **7,** 1289–1297
9. Warmka, J., Hanneman, J., Lee, J., Amin, D., and Ota, I. (2001) *Mol. Cell Biol.* **21,** 51–60
10. Albertyn, J., Hohmann, S., Thevelein, J. M., and Prior, B. A. (1994) *Mol. Cell Biol.* **14,** 4135–4144
11. Brewster, J. L., and Gustin, M. C. (1994) *Yeast* **10,** 425–439
12. Alexander, M. R., Tyers, M., Perret, M., Craig, B. M., Fang, K. S., and Gustin, M. C. (2001) *Mol. Biol. Cell* **12,** 53–62
13. Cyert, M. S., and Thorner, J. (1992) *Mol. Cell Biol.* **12,** 3460–3469
14. Nakamura, T., Liu, Y., Hirata, D., Namba, H., Harada, S., Hirokawa, T., and Miyakawa, T. (1993) *EMBO J.* **12,** 4063–4071
15. Mendoza, I., Rubio, F., Rodriguez-Navarro, A., and Pardo, J. M. (1994) J. *Biol. Chem.* **269,** 8792–8796
16. Farcasanu, I. C., Hirata, D., Tsuchiya, E., Nishiyama, F., and Miyakawa, T. (1995) *Eur. J. Biochem.* **232,** 712–717
17. Matheos, D. P., Kingsbury, T. J., Ahsan, U. S., and Cunningham, K. W. (1997) *Genes Dev.* **11,** 3445–3458
18. Stathopoulos, A. M., and Cyert, M. S. (1997) *Genes Dev.* **11,** 3432–3444
19. Garrett-Engele, P., Moilanen, B., and Cyert, M. S. (1995) *Mol. Cell Biol.* **15,** 4103–4114
20. Nakamura, T., Ohmoto, T., Hirata, D., Tsuchiya, E., and Miyakawa, T. (1996) *Mol. Gen. Genet.* **251,** 211–219
21. Mizunuma, M., Hirata, D., Miyahara, K., Tsuchiya, E., and Miyakawa, T. (1998) *Nature* **392,** 303–306
22. Cheng, A., Ross, K. E., Kaldis, P., and Solomon, M. J. (1999) *Genes Dev.* **13,** 2946–2957
23. Booher, R. N., Deshaies, R. J., and Kirschner, M. W. (1993) *EMBO J.* **12,** 3417–3426
24. Adams, A. E., and Pringle, J. R. (1991) *Methods Enzymol.* **194,** 729–731
25. Gaits, F., Shiozaki, K., and Russell, P. (1997) *J. Biol. Chem.* **272,** 17873–17879
26. Takekawa, M., Maeda, T., and Saito, H. (1998) *EMBO J.* **17,** 4744–4752
27. Lee, B. N., and Elion, E. A. (1999) *Proc. Natl. Acad. Sci. U. S. A.* **96,** 12679–12684
28. O'Rourke, S. M., and Herskowitz, I. (1998) *Genes Dev.* **12,** 2874–2886
29. Ma, X. J., Lu, Q., and Grunstein, M. (1996) *Genes Dev.* **10,** 1327–1340
30. McMillan, J. N., Sia, R. A., and Lew, D. J. (1998) *J. Cell Biol.* **142,** 1487–1499
31. Sia, R. A., Bardes, E. S., and Lew, D. J. (1998) *EMBO J.* **17,** 6678–6688
32. Tanida, I., Hasegawa, A., Iida, H., Ohya, Y., and Anraku, Y. (1995) *J. Biol. Chem.* **270,** 10113–10119
33. Cunningham, K. W., and Fink, G. R. (1996) *Mol. Cell Biol.* **16,** 2226–2237
34. Denis, V., and Cyert, M. S. (2002) *J. Cell Biol.* **156,** 29–34
35. Mazur, P., Morin, N., Baginsky, W., El-Sherbeini, M., Clemas, J. A., Nielsen, J. B., and Foor, F. (1995) *Mol. Cell Biol.* **15,** 5671–5681
36. Uesono, Y., and Toh-E, A. (2002) *J. Biol. Chem.* **277,** 13848–13855
37. Cruz, M. C., Fox, D. S., and Heitman, J. (2001) *EMBO J.* **20,** 1020–1032
38. Chang, H. Y., Takei, K., Sydor, A. M., Born, T., Rusnak, F., and Jay, D. G. (1995) *Nature* **376,** 686–690
39. Withee, J. L., Mulholland, J., Jeng, R., and Cyert, M. S. (1997) *Mol. Biol. Cell* **8,** 263–277
40. Withee, J. L., Sen, R., and Cyert, M. S. (1998) *Genetics* **149,** 865–878
41. Sagasti, A., Hisamoto, N., Hyodo, J., Tanaka-Hino, M., Matsumoto, K., and Bargmann, C. I. (2001) *Cell* **105,** 221–232
42. Lim, H. W., New, L., Han, J., and Molkentin, J. D. (2001) *J. Biol. Chem.* **276,** 15913–15919
43. Sakumoto, N., Mukai, Y., Uchida, K., Kouchi, T., Kuwajima, J., Nakagawa, Y., Sugioka, S., Yamamoto, E., Furuyama, T., Mizubuchi, H., Ohsugi, N., Sakuno, T., Kikuchi, K., Matsuoka, I., Ogawa, N., Kaneko, Y., and Harashima, S. (1999) *Yeast* **15,** 1669–1679